NASA/TM—2006-214350

Cyclic Oxidation Behavior of Cold Sprayed CuCrAl-Coated and Uncoated GRCop-84 Substrates for Space Launch Vehicles

S.V. Raj and C. Barrett
Glenn Research Center, Cleveland, Ohio

J. Karthikeyan
ASB Industries, Inc., Barberton, Ohio

R. Garlick
Glenn Research Center, Cleveland, Ohio

June 2006

NASA STI Program . . . in Profile

Since its founding, NASA has been dedicated to the advancement of aeronautics and space science. The NASA Scientific and Technical Information (STI) program plays a key part in helping NASA maintain this important role.

The NASA STI Program operates under the auspices of the Agency Chief Information Officer. It collects, organizes, provides for archiving, and disseminates NASA's STI. The NASA STI program provides access to the NASA Aeronautics and Space Database and its public interface, the NASA Technical Reports Server, thus providing one of the largest collections of aeronautical and space science STI in the world. Results are published in both non-NASA channels and by NASA in the NASA STI Report Series, which includes the following report types:

- TECHNICAL PUBLICATION. Reports of completed research or a major significant phase of research that present the results of NASA programs and include extensive data or theoretical analysis. Includes compilations of significant scientific and technical data and information deemed to be of continuing reference value. NASA counterpart of peer-reviewed formal professional papers but has less stringent limitations on manuscript length and extent of graphic presentations.

- TECHNICAL MEMORANDUM. Scientific and technical findings that are preliminary or of specialized interest, e.g., quick release reports, working papers, and bibliographies that contain minimal annotation. Does not contain extensive analysis.

- CONTRACTOR REPORT. Scientific and technical findings by NASA-sponsored contractors and grantees.

- CONFERENCE PUBLICATION. Collected papers from scientific and technical conferences, symposia, seminars, or other meetings sponsored or cosponsored by NASA.

- SPECIAL PUBLICATION. Scientific, technical, or historical information from NASA programs, projects, and missions, often concerned with subjects having substantial public interest.

- TECHNICAL TRANSLATION. English-language translations of foreign scientific and technical material pertinent to NASA's mission.

Specialized services also include creating custom thesauri, building customized databases, organizing and publishing research results.

For more information about the NASA STI program, see the following:

- Access the NASA STI program home page at *http://www.sti.nasa.gov*

- E-mail your question via the Internet to *help@sti.nasa.gov*

- Fax your question to the NASA STI Help Desk at 301–621–0134

- Telephone the NASA STI Help Desk at 301–621–0390

- Write to:
  NASA STI Help Desk
  NASA Center for AeroSpace Information
  7121 Standard Drive
  Hanover, MD 21076–1320

NASA/TM—2006-214350

Cyclic Oxidation Behavior of Cold Sprayed CuCrAl-Coated and Uncoated GRCop-84 Substrates for Space Launch Vehicles

S.V. Raj and C. Barrett
Glenn Research Center, Cleveland, Ohio

J. Karthikeyan
ASB Industries, Inc., Barberton, Ohio

R. Garlick
Glenn Research Center, Cleveland, Ohio

National Aeronautics and
Space Administration

Glenn Research Center
Cleveland, Ohio 44135

June 2006

Acknowledgments

The authors thank David Ellis for supplying the GRCop-84 substrates used in this research and James Nesbitt for analyzing the composition of the discoloration on the HIPed coatings and for his helpful comments. This research was funded by NASA's Space Transportation Program.

Level of Review: This material has been technically reviewed by technical management.

Available from

NASA Center for Aerospace Information
7121 Standard Drive
Hanover, MD 21076–1320

National Technical Information Service
5285 Port Royal Road
Springfield, VA 22161

Available electronically at http://gltrs.grc.nasa.gov

Cyclic Oxidation Behavior of Cold Sprayed CuCrAl-Coated and Uncoated GRCop-84 Substrates for Space Launch Vehicles

S.V. Raj and C. Barrett
National Aeronautics and Space Administration
Glenn Research Center
Cleveland, Ohio 44135

J. Karthikeyan
ASB Industries, Inc.
Barberton, Ohio 44203–1689

R. Garlick
National Aeronautics and Space Administration
Glenn Research Center
Cleveland, Ohio 44135

Abstract

A newly developed Cu-23 (wt %) Cr-5%Al (CuCrAl) alloy shown to resist hydridation and oxidation in an as-cast form is currently being considered as a protective coating for GRCop-84, which is an advanced copper alloy containing 8 (at.%) Cr and 4 (at.%) Nb. The coating was deposited on GRCop-84 substrates by the cold spray deposition technique. Cyclic oxidation tests conducted in air on both coated and uncoated substrates between 773 and 1073 K revealed that the coating remained intact and protected the substrate up to 1073 K. No significant weight loss of the coated specimens were observed at 773 and 873 K even after a cumulative cyclic time of 500 h. About a 10 percent weight loss observed at 973 and 1073 K was attributed to the excessive oxidation of the uncoated sides. In contrast, the uncoated substrate lost as much as 80 percent of its original weight under similar test conditions. It is concluded that the cold sprayed CuCrAl coating is suitable for protecting GRCop-84 substrates.

1. Introduction

The National Aeronautics and Space Administration (NASA) has been developing technologies for a new generation of advanced launch vehicles in its efforts to increase its future heavy lift capacity in a more reliable and economical manner compared to the Space Shuttle. The latter vehicle uses the state-of-the-art in liquid propellant rocket engine design and it is the only operating reusable launch vehicle (RLV) in the world. Therefore, all technological developments for future RLV rocket engines will be compared against the Space Shuttle Main Engine (SSME), which naturally forms the baseline for such comparisons. The SSME operates under extremely severe conditions with a chamber pressure of about 20 MPa, a throat wall temperature of about 840 K, a throat heat flux varying between 130 and 150 MW m^{-2} and an expected life of 55 thermal cycles (refs. 1 to 3). Engines for more advanced concepts, such as orbital transfer vehicles, are expected to last 200 to 300 thermal cycles (ref. 1).

Combustion liner materials in a rocket engine experience extreme conditions due to a combination of environmental and thermo-mechanical effects. The hot wall side of the liner is exposed to combustion flame temperatures of about 3600 K (ref. 2) while the cold wall side of the liner experiences cryogenic liquid hydrogen (LH_2) temperatures of 20 K. Copper and its alloys have been traditionally used as combustor liner materials in these regenerative rocket engines because of their high thermal conductivity which enables an efficient heat transfer from the combustion flame to preheat the cryogenic LH_2 flowing

in the cooling channels. Considering that the wall thickness between the cold and hot surfaces of the combustor liner material is typically 1 mm (ref. 1), it is evident that large transient thermal gradients are established across the liner cross-section. As a result, the liner hot wall experiences large thermal plastic cyclic strains during each mission cycle leading to plastic deformation and cracking of the cooling passages during the life of the combustor liner (refs. 3 to 6). The process is further complicated by the environmental degradation of the uncoated copper alloy liners due to a combination of the spallation of the copper oxide scale and "blanching," which consists of repeated oxidation of the copper matrix and subsequent reduction of the oxide scale (ref. 6). As a result, the initially highly polished interior surface of the combustion liner becomes progressively rougher and thinner leading to web formation during the service life of the engine. Thus, the liner material can become structurally weakened unable to carry the mechanical loads, while also exhibiting a diminished heat transfer capability across the liner walls thereby resulting in the development of hot spots.

The design of the next generation of reusable launch vehicles is likely to use GRCop-84 (Cu-8 (at.%) Cr-4%Nb) copper alloy liners based on a composition invented at NASA Glenn Research Center (GRC) (ref. 7). Many of the properties of this alloy have been shown to be far superior to other conventional copper alloys, such as NARloy-Z, which are currently being used as combustor liners in rocket engines (refs. 7 to 9). The application of protective coatings on GRCop-84 and other copper alloy substrates can minimize or eliminate many of the problems experienced by uncoated liners and significantly extend their operational lives. This factor potentially translates to increased component reliability, shorter depot maintenance turn around time and lower operational cost. In addition, the use of a suitable top coat to act as a thermal barrier can allow the engine to run at higher temperatures thereby resulting in its increased thermal efficiency. As a result, several types of ceramic (refs. 1 and 5) and metallic (refs. 10 to 13) coatings have been advocated as protective coatings for copper alloy liners.

The present study was undertaken as part of a larger investigation to develop and characterize suitable coatings and deposition techniques for GRCop-84 for liquid propulsion rocket engines. This paper discusses the protective capabilities of a newly developed Cu-23 (wt %) Cr-5%Al[1] (CuCrAl) coating alloy deposited by the cold spray deposition technique (refs. 14 and 15). The oxidation properties of this alloy in the as-cast and annealed condition were shown to be far superior to several Cu-Cr alloys (ref. 16).

2. Experimental Procedures

The CuCrAl coating alloy was procured from Crucible Research, Inc., Pittsburgh, Pennsylvania, as gas atomized powder. Scanning electron microscopy (SEM) images of the powder particles revealed that they generally possessed a spherical morphology (fig. 1). The average particle size, analyzed by a Beckman Coulter Rapid-Vue particle size analyzer, was 15 ± 5 μm. The coating was cold sprayed on GRCop-84 substrates of varying shapes and dimensions, where the coating was golden-yellow in the as-sprayed condition (fig. 2). The oxidation disk specimens were 12.7 mm in diameter and 2 mm thick with 1.5 mm diameter holes located about 1.5 mm from an edge. These holes allowed each specimen to be hung vertically in a furnace from hooked ceramic-shielded Pt wires. These specimens were sprayed on both faces but the edges remained uncoated. Several rectangular and square specimens approximately 25.4 x 25.4 x 3.2 mm in dimensions were coated on one side primarily for microstructural observations. All specimens were hot isostatically pressed (HIP) in batches under proprietary conditions to consolidate the coatings. In some cases, the coatings were found to have been contaminated during HIP leading to a dark coloration of the as-sprayed golden-colored coating. Energy dispersive analysis (EDS) of some of the coated specimens revealed oxygen, silicon and potassium peaks in these coatings. The effects of these contaminants did not appear to have any noticeable influence on the observations reported here.

[1]Unless otherwise stated, all compositions reported in this paper are in wt %.

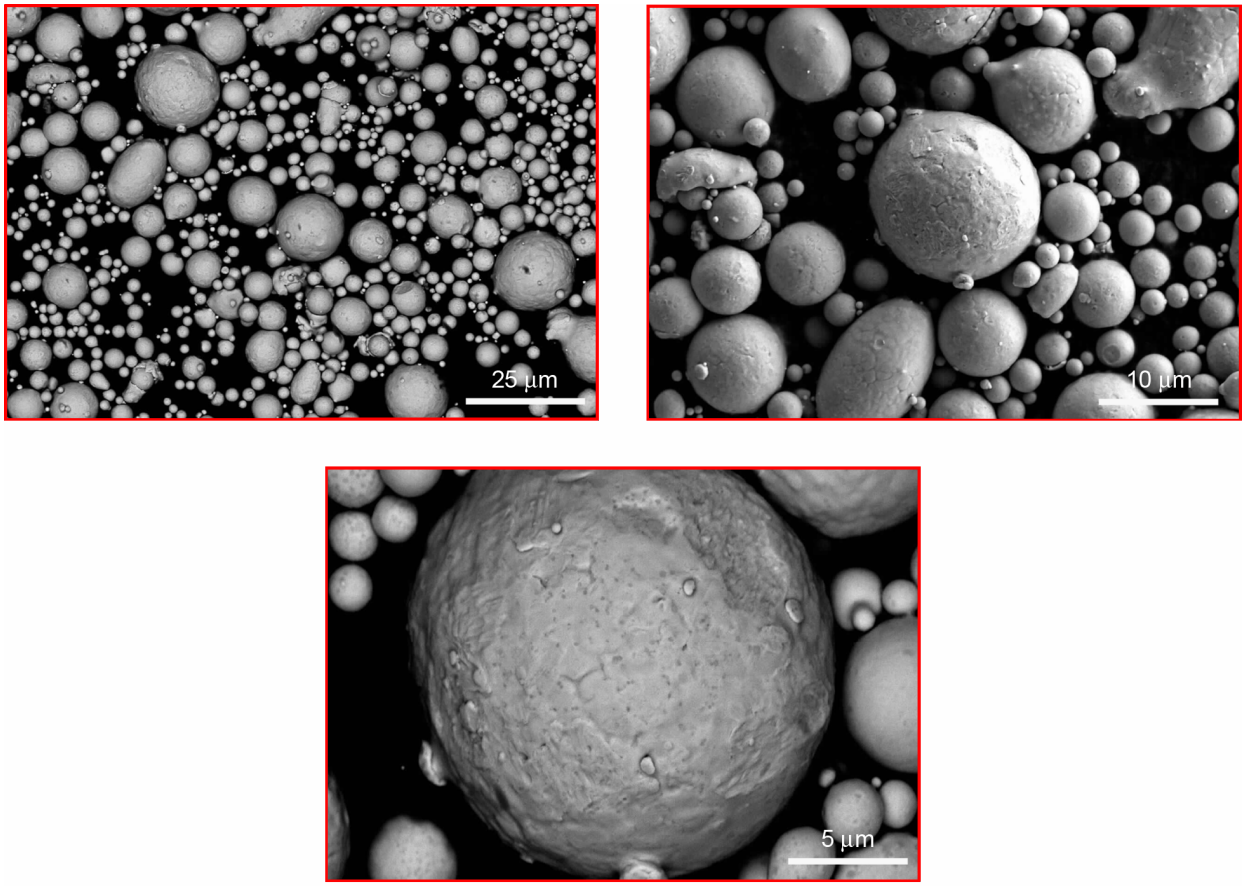

Figure 1.—Scanning electron micrographs showing the morphology of the as-sprayed CuCrAl powder. The average particle size is 15 ± 5 µm.

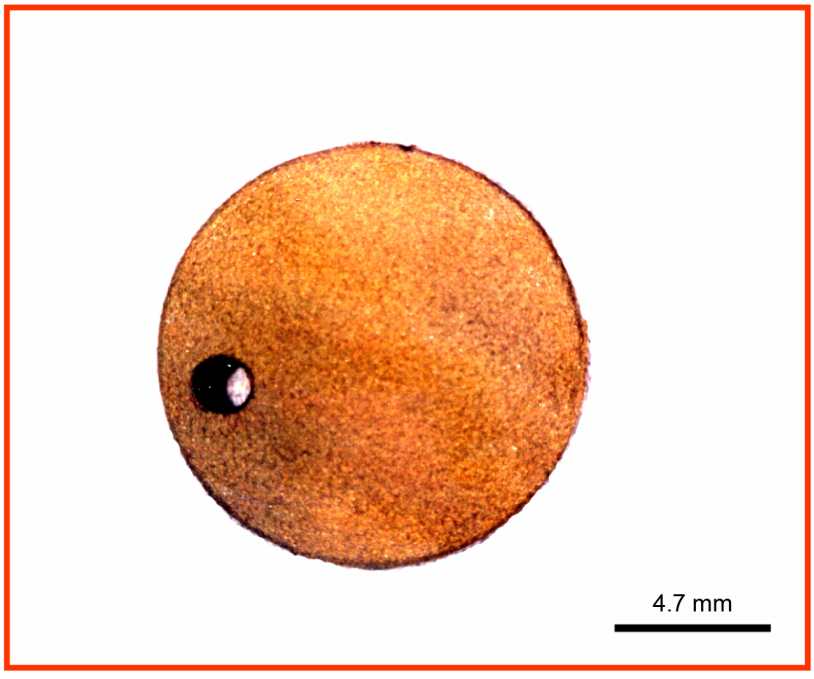

Figure 2.—Macrograph of a CuCrAl cold sprayed cyclic oxidation specimen.

Cyclic oxidation tests were conducted in air between 773 and 1073 K, where the specimens were held at temperature for 1800 s followed by a natural cool down to ambient within 300 s. Each coated specimen was cycled along with an uncoated sample in the same furnace to ensure that the observations are comparable under similar conditions. The coated and uncoated specimens were introduced into a vertical multiple tube furnace maintained at the desired temperature and automatically cycled for a predetermined number of cycles prior to weighing them to evaluate the degree of weight change. The specimens were hung from Pt wires and centered coaxially with the axes of the furnace tubes using a set of slotted steel guides placed at the top of each tube. This procedure ensured that both faces and edges of the specimens were uniformly heated in the furnace. Since an individual thermocouple could not be attached to each specimen to monitor its actual temperature during the course of the test, the temperature within each tube was measured at the appropriate depth and compared with the reading of the control thermocouple. The controller set point was adjusted until the measured temperature was within 5 K of the control thermocouple reading, which was maintained at the desired temperature. The output from the control thermocouple was monitored by a data logging system, which displayed a plot of temperature versus time over the duration of the test. The oxidized specimens were periodically examined and photographed at low magnifications to record time dependent morphological changes of the coated and the uncoated surfaces. The compositions of specimen surfaces and spalled oxide scale were also periodically analyzed by x-ray diffraction (XRD). The tested and untested specimens were characterized by optical, scanning electron (SE), back scattered electron (BSE) microscopies and energy dispersive spectroscopy (EDS). The BSE, EDS, and SE analyses were conducted using a high resolution field emission (FE) scanning electron microscope (SEM). The coating thickness of several as-sprayed and HIPed specimens were measured on photographs of the polished cross-sections along random test lines. The errors in measurement reported in this paper represent the 95 percent confidence limits.

3. Results and Discussion

3.1 Microstructural Characterization of As-Sprayed and HIPed Specimens

An examination of the polished cross-sections of as-sprayed and HIPed specimens revealed specimen-to-specimen variation in the quality of the coating density and thickness. The coating consisted of a two phase microstructure consisting of a dark β-Cr phase and a light (Cu, Al) matrix. Since most of the Al was in solid solution, the effective composition of the matrix was estimated to be about Cu-6.5%Al. The coatings in many specimens were dense and almost crack and void free with few voids at the coating-substrate interfaces (fig. 3(a) and (b)). However, many other specimens showed extensive cracks and voids (fig. 3(c)). All specimens showed embedded grit in several regions of the substrate close to its interface with the coating (fig. 3(d)). Clearly, the spray parameters and procedures need to be further optimized to improve coating quality in a reproducible manner.

Visual inspection of the coated surfaces often showed a rastered appearance corresponding to the spray direction (fig. 2). In many instances, the cross-sectional microstructures also revealed large variations in coating thickness along the field of view. Measurements of the coating thickness on several specimens revealed a batch-to-batch variation. These thickness variations exhibited a bimodal distribution, where the averages of these distributions were 263 ± 3 μm and 613 ± 7 μm (fig. 4). The observation of these variations in the coating thickness suggests non-uniform deposition of the powder during spraying. This non-uniformity can be caused by one or more factors, such as interrupted spraying due to nozzle clogging, uneven rate of powder flow from the hopper to the spray gun and a mismatch between the rotational speed of the specimen and the lateral traverse speed of the spray gun. Once again, additional process parametric studies need to be undertaken in order to minimize variations in the coating thickness to acceptable values.

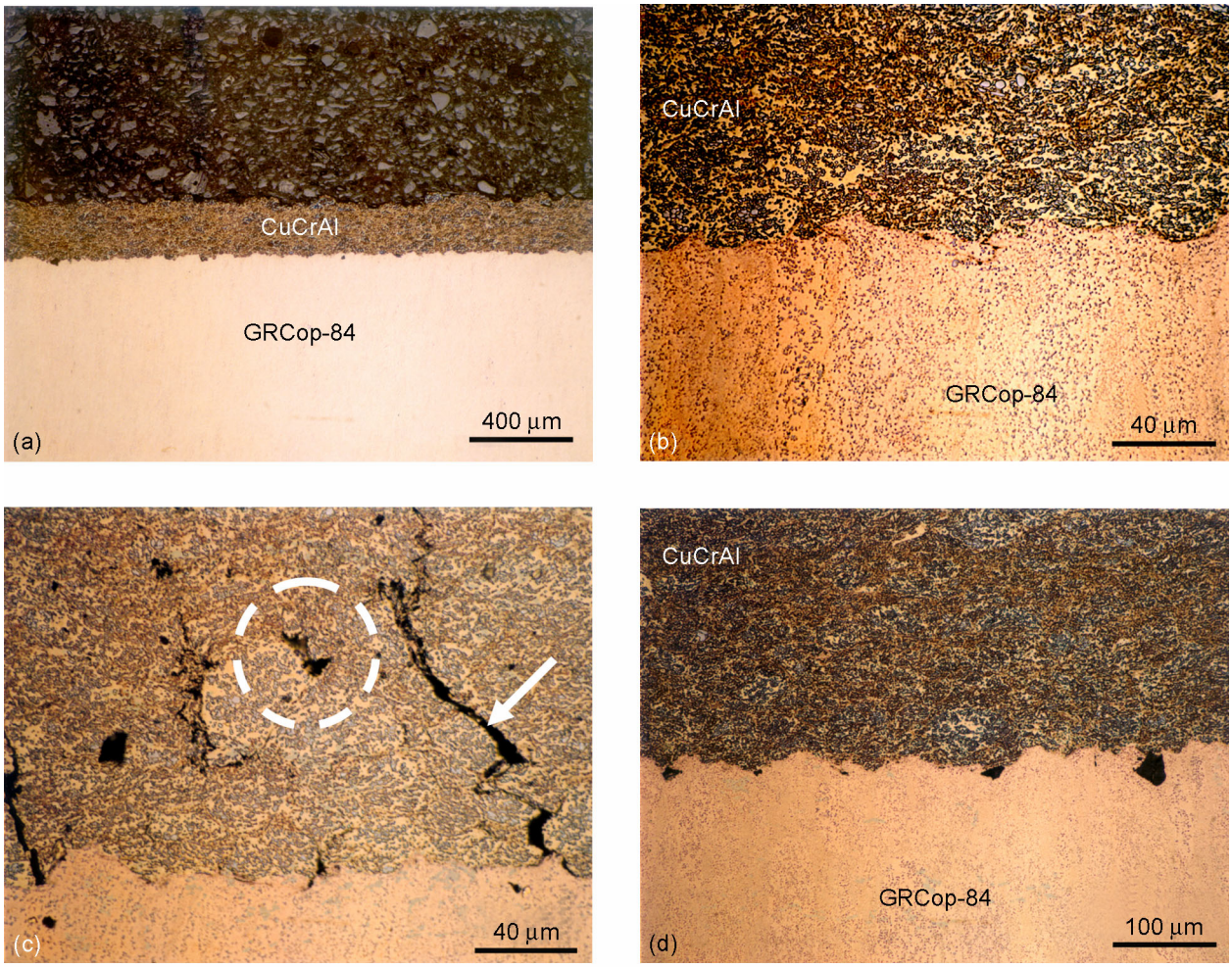

Figure 3.—(a) Low and (b) high magnification optical micrographs showing defect-free coatings. Optical micrographs showing (c) cracks (e.g. arrow) and voids (e.g. circle); and (d) embedded alumina grit in the substrate.

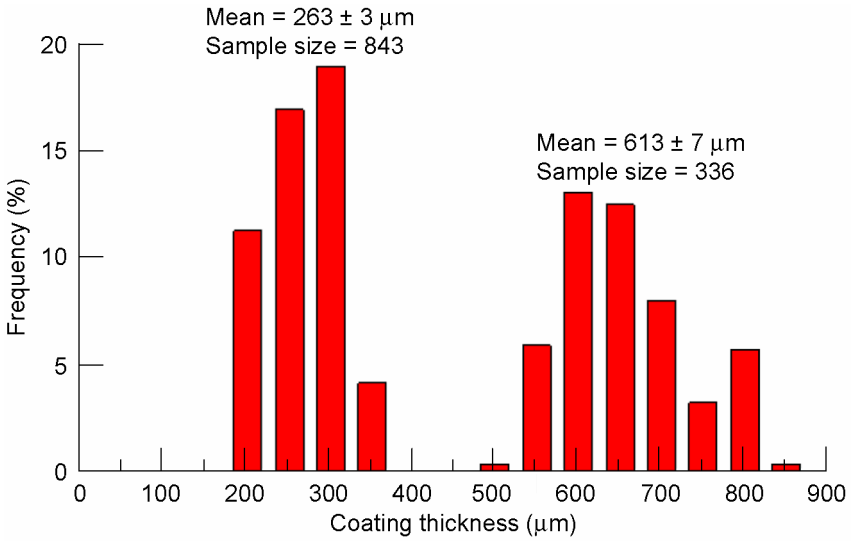

Figure 4.—Batch-to-batch bimodal distribution in the coating thickness of the cold sprayed CuCrAl-coated GRCop-84 specimens.

3.2 Cyclic Oxidation

Figure 5(a) shows the variation of the instantaneous weight, W, normalized by the initial weight, W_0, with cumulative cyclic time, t, for the coated and uncoated specimens cycled at 773 K. Clearly, the coated specimen shows negligible weight loss at this temperature as compared to the uncoated GRCop-84, which has lost about 60 percent of its weight after 500 h corresponding to 1000 cycles. Macrographs of the coated specimen before (fig. 5(b)) and after (fig. 5(c)) testing revealed that the coating was still intact although it showed some degree of discoloration presumably due to oxidation. In contrast, the uncoated GRCop-84 had undergone extensive oxidation and scale spallation leading to a considerable loss in weight (fig. 5(d)).

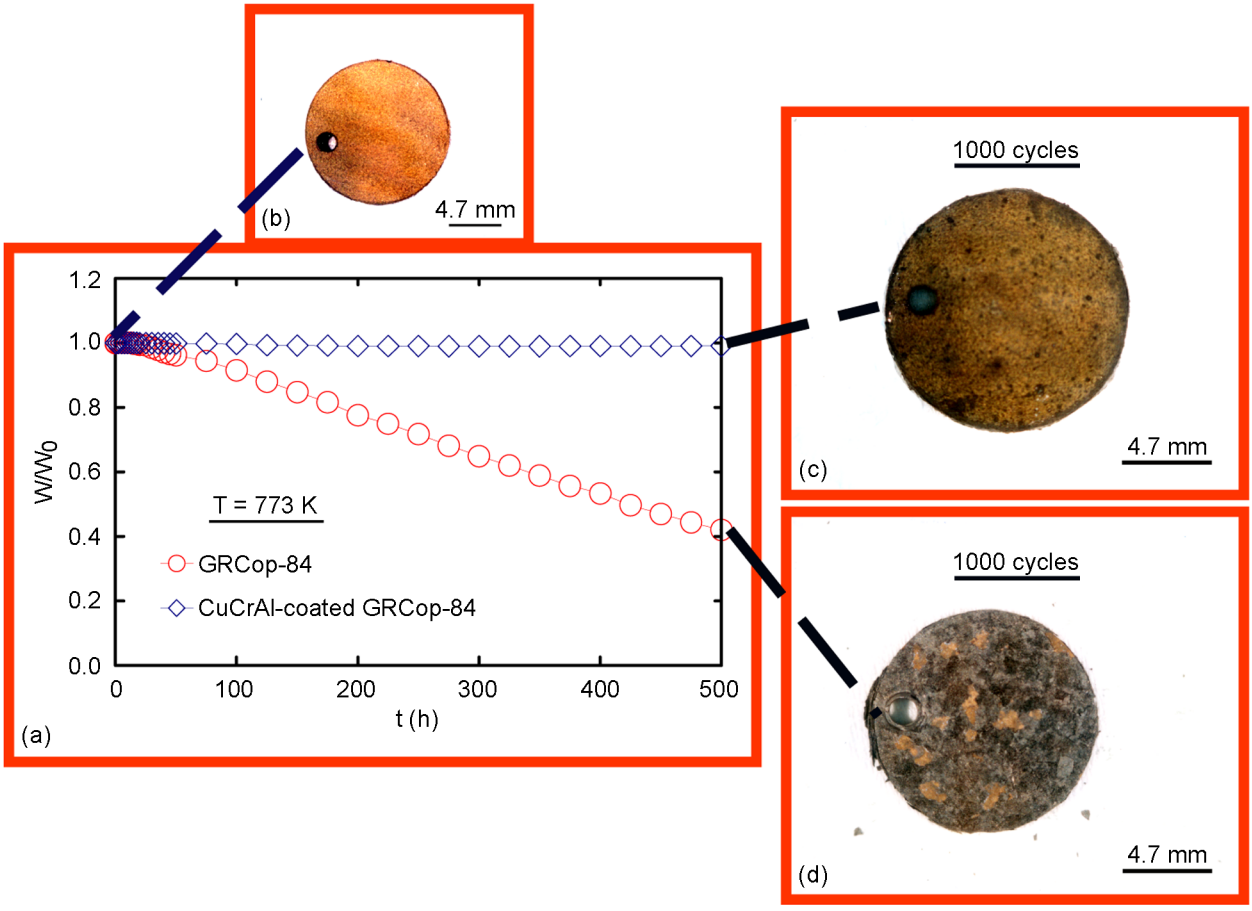

Figure 5.—(a) Comparison of the normalized weight change versus cumulative cyclic time for coated and uncoated GRCop-84 substrates at 773 K. Optical macrographs of (b) unexposed, and (c) coated and (d) uncoated specimens after 1000 cycles.

Figures 6(a), 7(a), and 8(a) show the normalized weight change data for the coated and uncoated GRCop-84 specimens cycled at 873, 973, and 1073 K, respectively. The corresponding macrographs of the tested and untested specimens are also shown in each figure as (b), (c), and (d). Once again, it is evident that the coated specimens have performed extremely well relative to the uncoated samples with the coating still intact at 1073 K. At 873 K, the uncoated specimen lost about 20 percent of its initial weight after 250 h corresponding to 500 cycles (fig. 6(a)). In contrast, the coated specimen showed no significant loss in weight. Once again, the coating was intact (fig. 6(c)) whereas the uncoated GRCop-84 showed extensive oxidation and scale spallation (fig. 6(d)). As evident in figure 5(a) and 6(a), the weight loss is significantly higher for the uncoated GRCop-84 at 773 K than at 873 K contrary to expected behavior. Since this observation was confirmed from repeat tests, it appears that this is a characteristic of the oxidation behavior of this alloy. Although the precise reason for this observed behavior is unclear, it appears to be related to the increased tenacity of the oxide scale with increasing temperature as discussed later. At 973 K, the differences between the coated and the uncoated substrates are stark with the uncoated specimen losing as much as about 70 percent of its weight after 75 h (fig. 7(a)) due to severe oxidation and spallation (fig. 7(d)). The coated specimen lost about 10 percent of its original weight after 500 h or 1000 cycles primarily due to the oxidation of the uncoated edges (fig. 7(c)). Remarkably, the coating performed reasonably well even at 1073 K although in this case the test had to be terminated prematurely after 80 cycles due to substantial oxidation of the uncoated edges (fig. 8(a) and (c)). Not surprisingly, the uncoated specimen showed extensive oxidation and cracking of the scale after 35 cycles at this temperature.

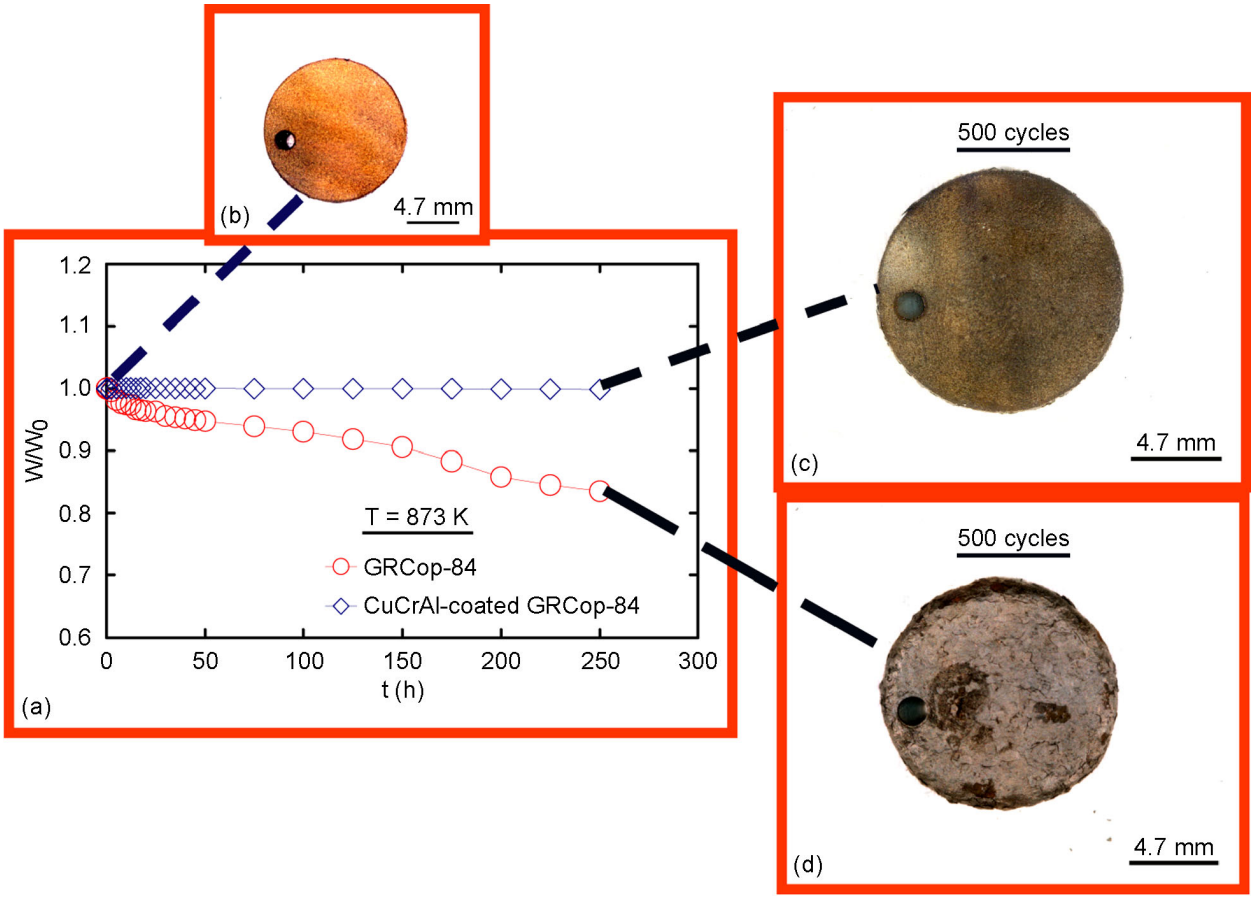

Figure 6.—(a) Comparison of the normalized weight change versus cumulative cyclic time for coated and uncoated GRCop-84 substrates at 873 K. Optical macrographs of (b) unexposed, and (c) coated and (d) uncoated specimens after 500 cycles.

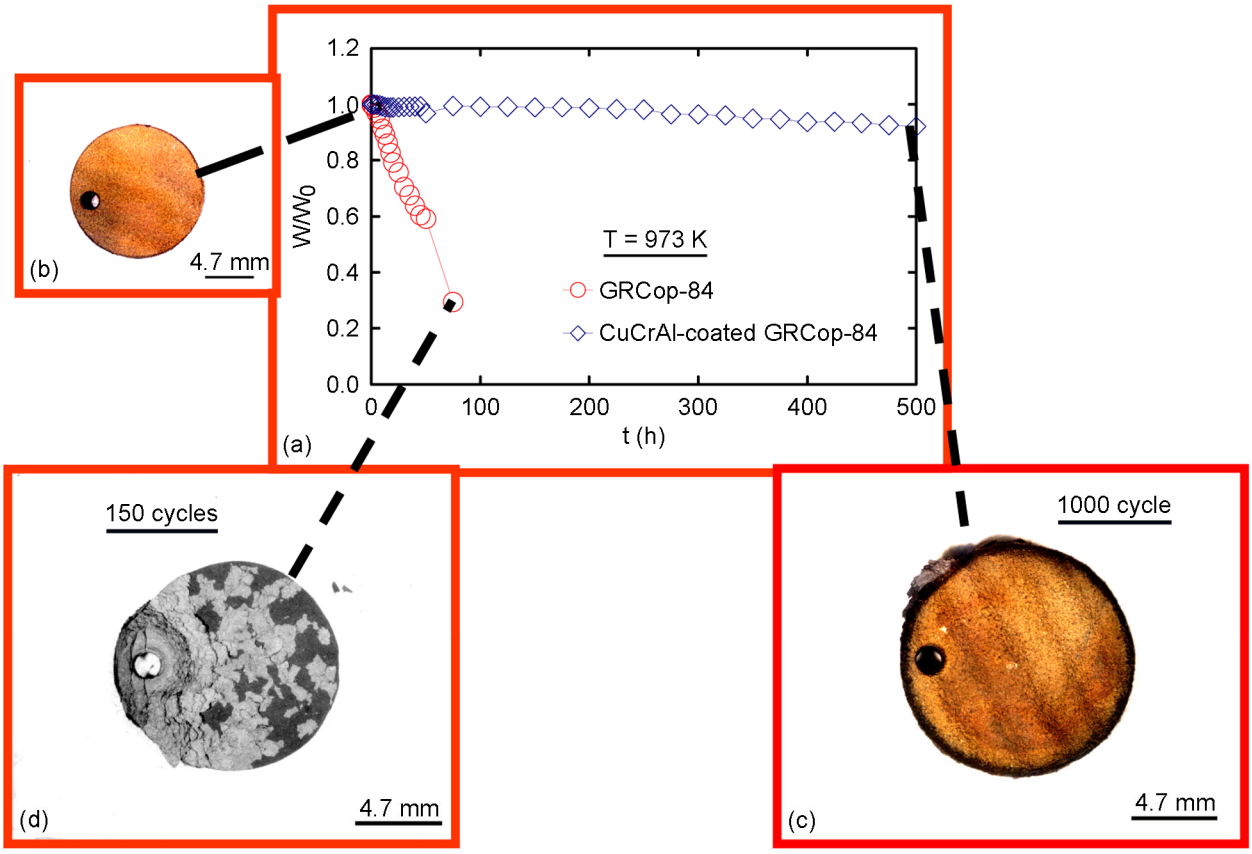

Figure 7.—(a) Comparison of the normalized weight change versus cumulative cyclic time for coated and uncoated GRCop-84 substrates at 973 K. Optical macrographs of (b) unexposed, and (c) coated and (d) uncoated specimens after 1000 and 150 cycles, respectively.

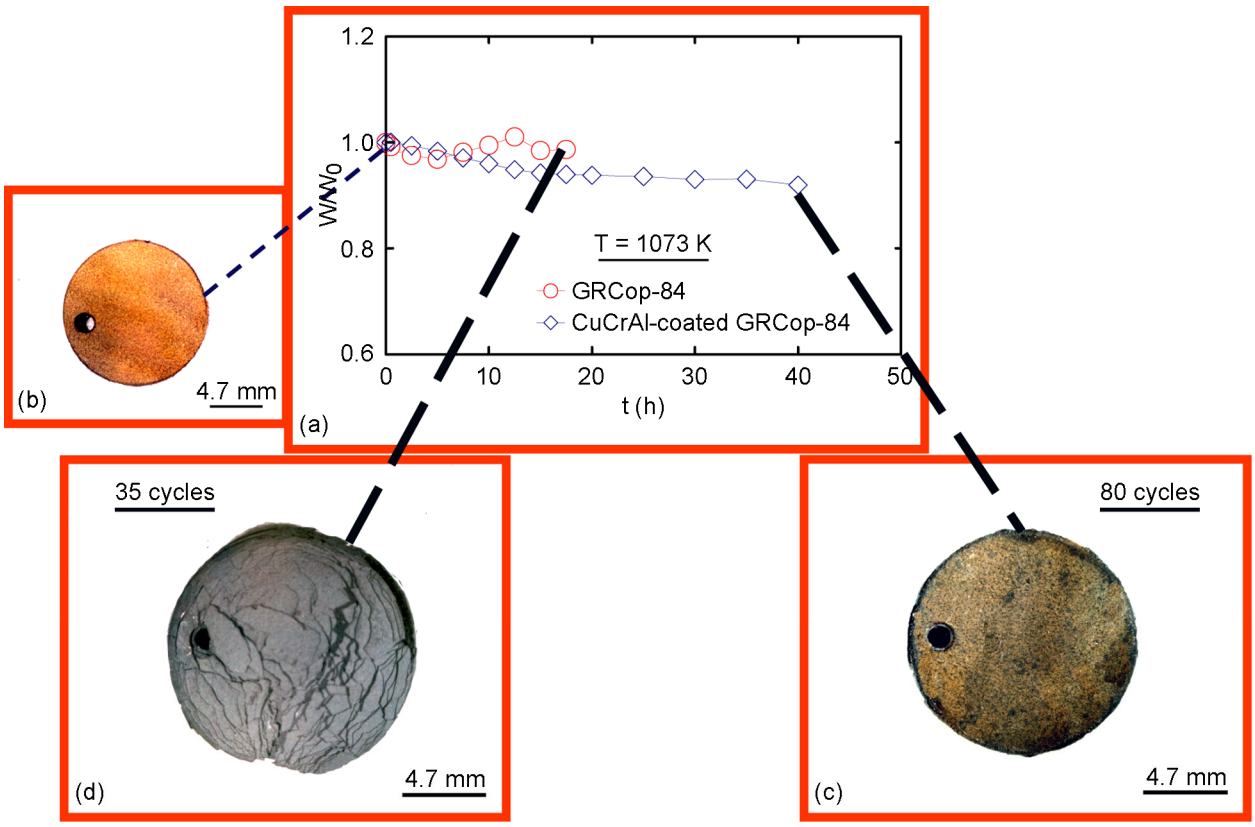

Figure 8.—(a) Comparison of the normalized weight change versus cumulative cyclic time for coated and uncoated GRCop-84 substrates at 1073 K. Optical macrographs of (b) unexposed, and (c) coated and (d) uncoated specimens after 80 and 35 cycles, respectively.

3.3 Microstructures of Oxidized Specimens

Figure 9(a) and (b) show the cross-sectional optical microstructures of the uncoated GRCop-84 specimen cyclically oxidized at 773 K for 1000 cycles at low and high magnifications, respectively. Most of the oxide scale has spalled off from the surface leaving behind bare metal susceptible to further oxidation (fig. 9(b)). The BSE image of the oxide scale showed alternating bands of dark and light layers with entrapped white particles (fig. 9(c)). The poor adhesion of the scale to the substrate is clearly evident in figure 9(b) and (c). An EDS analyses of the dark (region A) and light (region B) layers as well as the particles (region C) showed that the two layers were copper oxides with different oxygen content whereas the particles were rich in Cr, Cu, and Nb (fig. 9(d)). It is reasonable to conclude that the outer darker layer is CuO while the inner lighter layer is Cu_2O and the particles are Cr_2Nb originally present in the GRCop-84 alloy. The detection of a relatively strong oxygen peak in the EDS patterns from the Cr_2Nb particles (fig. 9(d)) indicate that they were oxidized, which is consistent with previous suggestion relating to the isothermal oxidation behavior of GRCop-84 (ref. 17). Two interesting observations may be noted. First, the darker outer CuO layer is denser than the lighter inner Cu_2O layer (fig. 9(c) and (d)). Second, well-rounded voids were often observed associated with the white particles (fig. 9(d)).

In contrast, the oxide scale on the uncoated specimen oxidized at 873 K for 500 cycles is largely intact over a substantial area of the sample despite extensive cracking (fig. 10(a) and (b)). These observations suggest that the scale is more tenacious at 873 than at 773 K, which is consistent with the observed differences in the weight change data shown in figures 5(a) and 6(a). A close examination of the

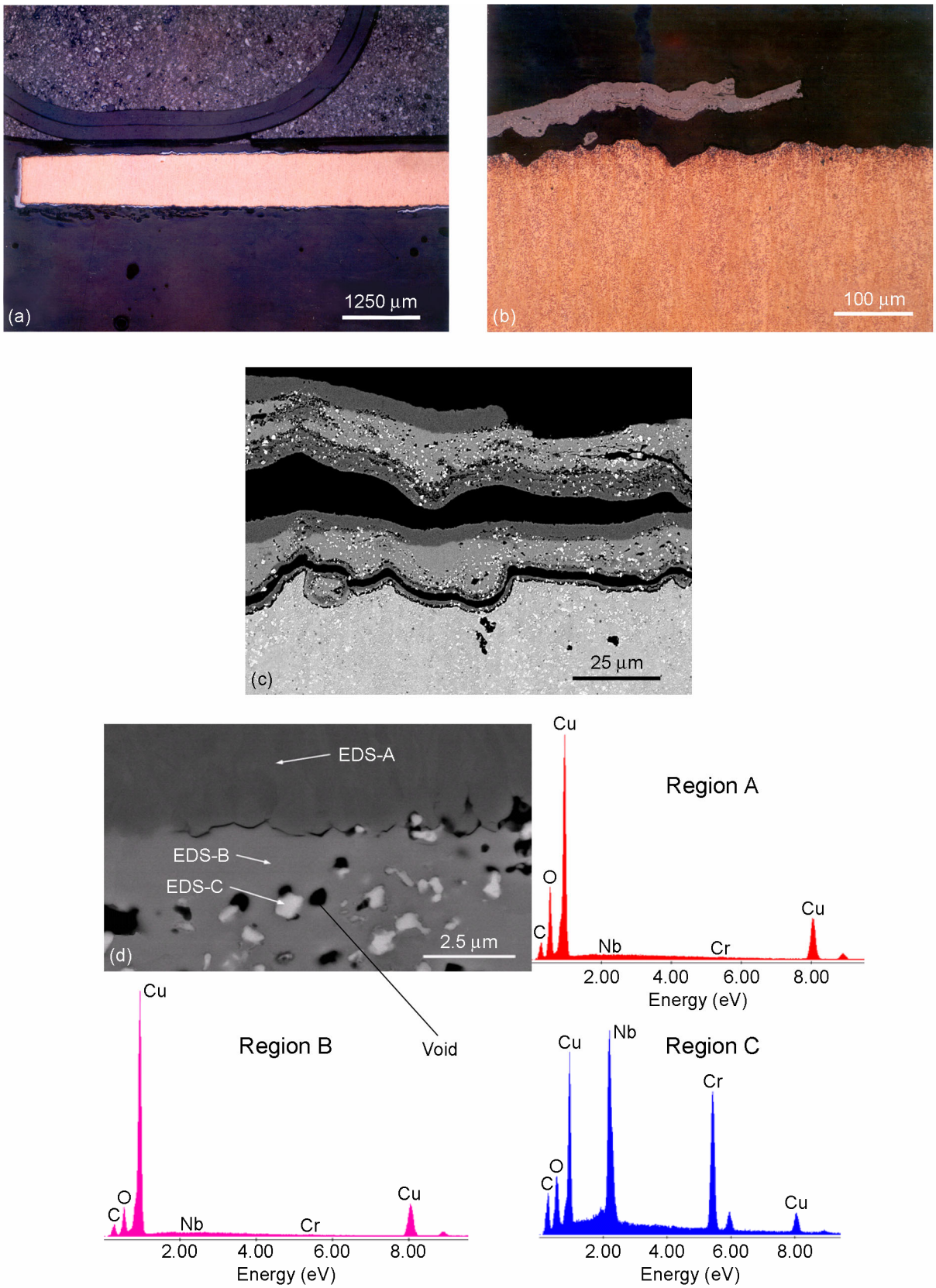

Figure 9.—(a) and (b) Optical microstructures and (c) and (d) back scattered electron images of the cross-section of the GRCop-84 specimen cyclically oxidized at 773 K for 1000 cycles. The EDS patterns are also shown in (d).

nature of the oxide scale showed that it consisted of several alternating layers of columnar and equiaxed grains (fig. 10(b)). The observation of columnar grains, which is visible mainly in regions in contact with the free surface, suggests that these had formed first due to the directional growth of single crystals of the copper oxide before transforming later on to the equiaxed granular microstructure observed in the subsequent layers. Similar morphologies are observable in the microstructures reported by Chiang and Grimmett (ref. 17) after isothermal oxidation of GRCop-84 at 1089 K. In this case, it was reported that there was a transition from CuO to Cu_2O to mixed oxides from the external surface to the interior.

The cross-sectional microstructure of the uncoated specimen tested at 1073 K for 35 cycles revealed extensive oxidation of the sample. Once again, the scale appears to be tenacious forming several layers with each layer approximately corresponding to a single cycle (fig. 11(a)). In this case, the outer layers were significantly more bent than the inner layers closer to the unoxidized GRCop-84 substrate due to an increase in the tensile stress component (fig. 11(b)). At high magnifications, these layers showed distinct separation between individual layers although there were some regions, where they were fused (fig. 11(c)). Interestingly, the thickness of each layer was uniform thereby suggesting that the rate of oxidation of the matrix and the rate of spallation of the oxide scale had achieved a steady-state condition. A close examination of the matrix revealed internally oxidized regions with the oxidation of the substrate first occurring with the formation of long oxide stringers (fig. 11(d)). Further oxidation of the matrix between adjacent stringers results in an increase in the density of the oxide scale.

Figure 12(a) to (d) show the cross-sectional microstructures of the coated specimen cycled at 773, 873, 973, and 1073 K. The non-uniform thickness of the coatings is evident in these figures (fig. 12(a) and (b)). There was no evidence of coating delamination in any of the thermally cycled specimens in these microstructures although the uncoated edges had oxidized to different degrees depending on the test temperature. Interestingly, the regions of the substrate at the uncoated edges in the vicinity of the coating-substrate interfaces appear to be more resistant to oxidation as compared to those close to the longitudinal axis of the specimen judging from the lack of any significant oxide scale. Presumably, this is due to Al diffusion from the coating into the matrix across the interfaces, which is expected to improve the oxidation resistance of the substrate. However, elemental image dot maps of regions showing the coating, the substrate and the interface revealed insignificant Al diffusion across the interface at 1073 K after 40 h and any observed Al rich region corresponded to embedded grit in the substrate (fig. 13). In fact, a close examination of figure 13 reveals that the oxygen-rich regions closely correspond to the α-Cr particles thereby suggesting the formation of dense islands of chromia during oxidation.

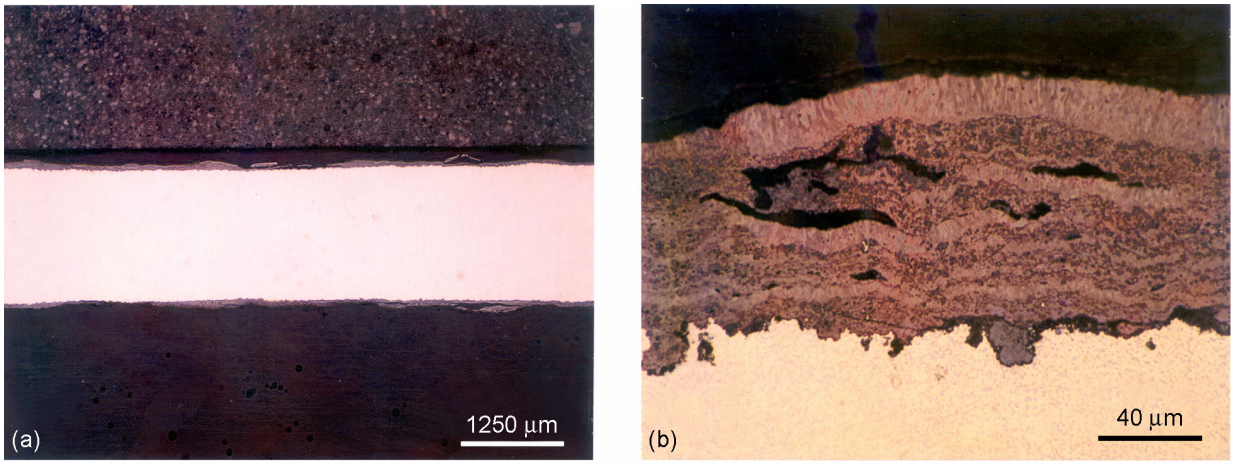

Figure 10.—(a) Low and (b) high magnification optical microstructures of the cross-section of the GRCop-84 specimen cyclically oxidized at 873 K for 500 cycles.

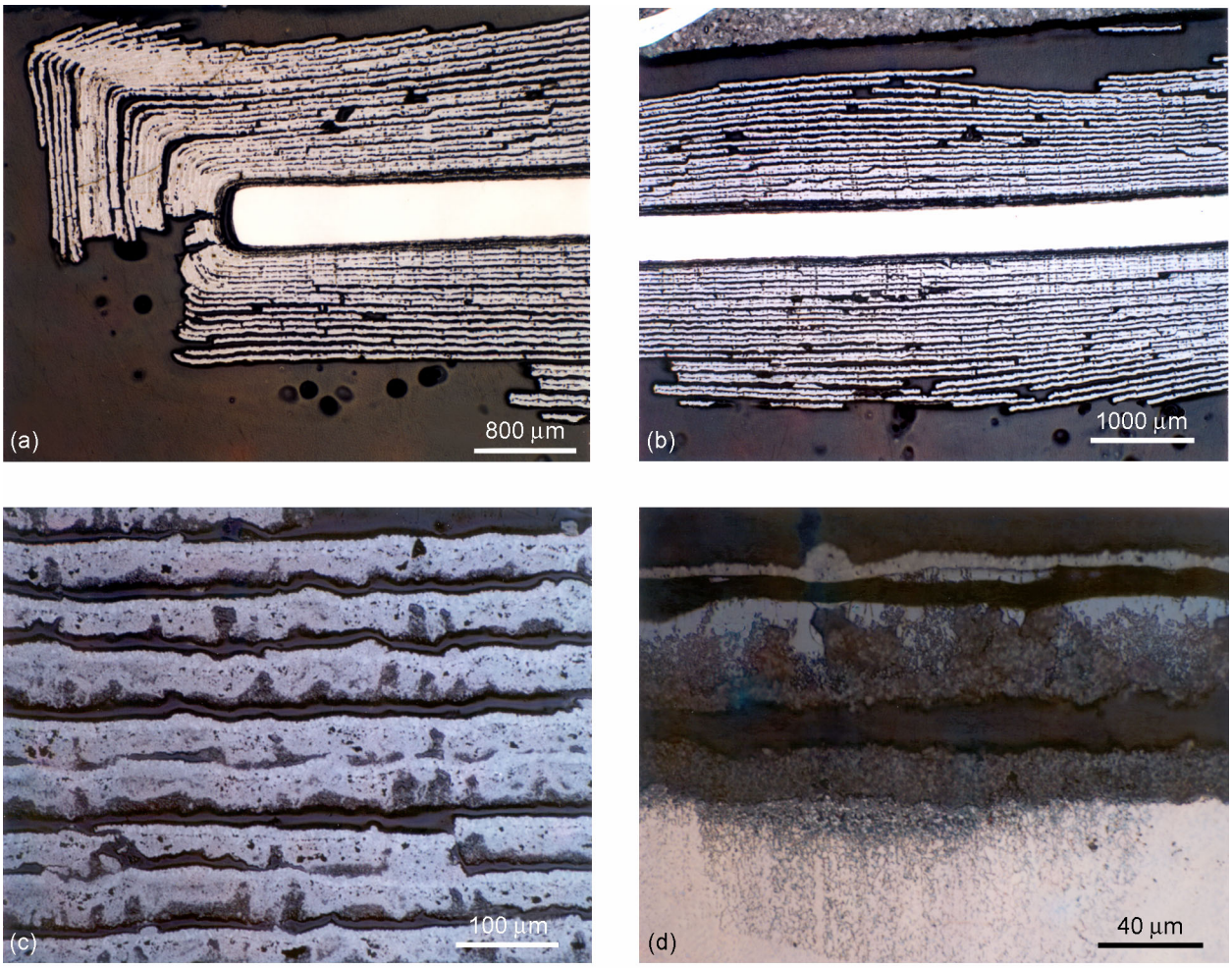

Figure 11.—(a-d) Optical micrographs of the cross-section of the GRCop-84 specimen cyclically oxidized at 1073 K for 35 cycles.

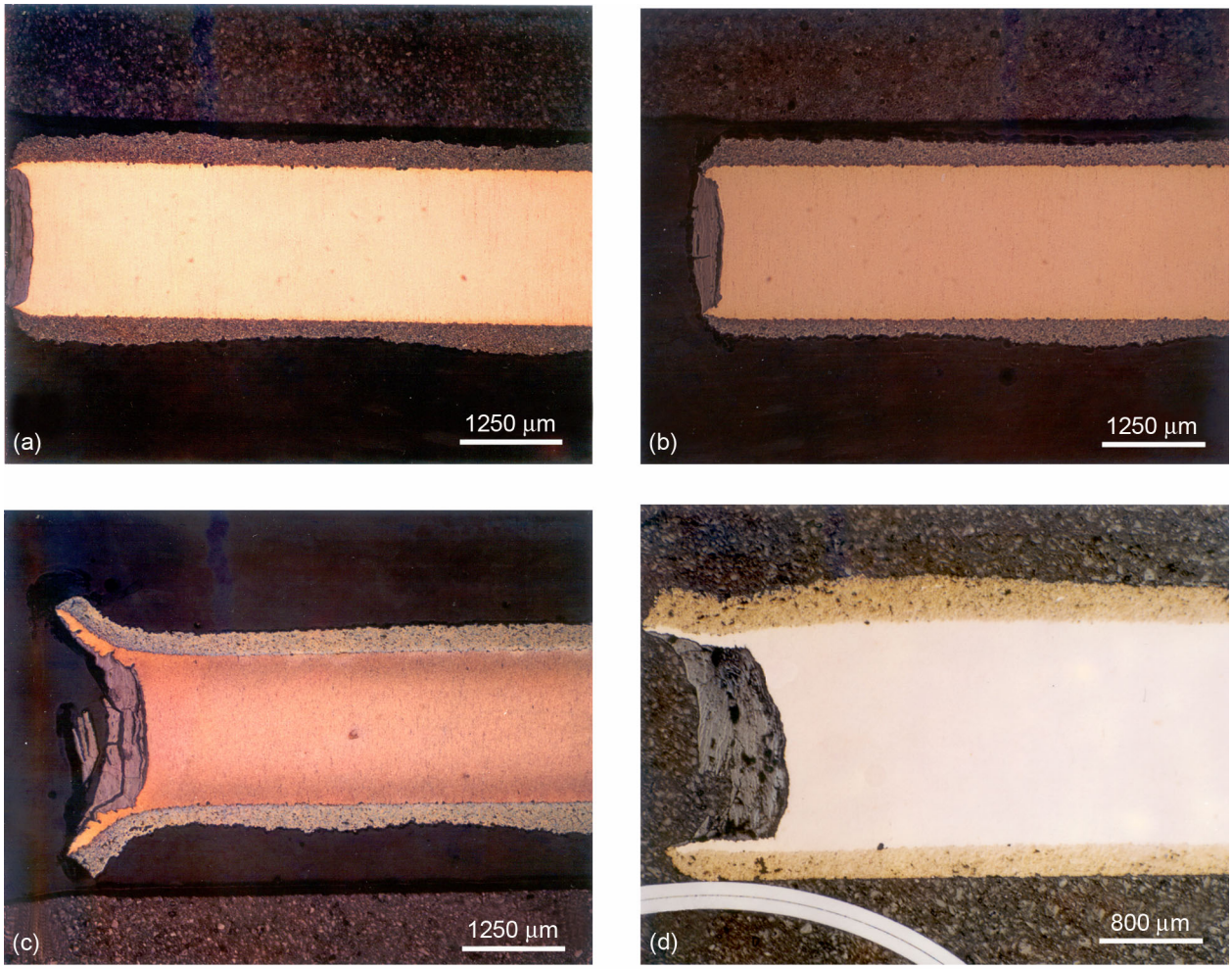

Figure 12.—Optical micrographs of the cross-sections the cold sprayed Cu-23Cr-5Al coated GRCop-84 specimens cyclically oxidized at (a) 773 K, 1000 cycles(b) 873 K, 500 cycles (c) 973 K, 1000 cycles and (d) 1073 K, 80 cycles.

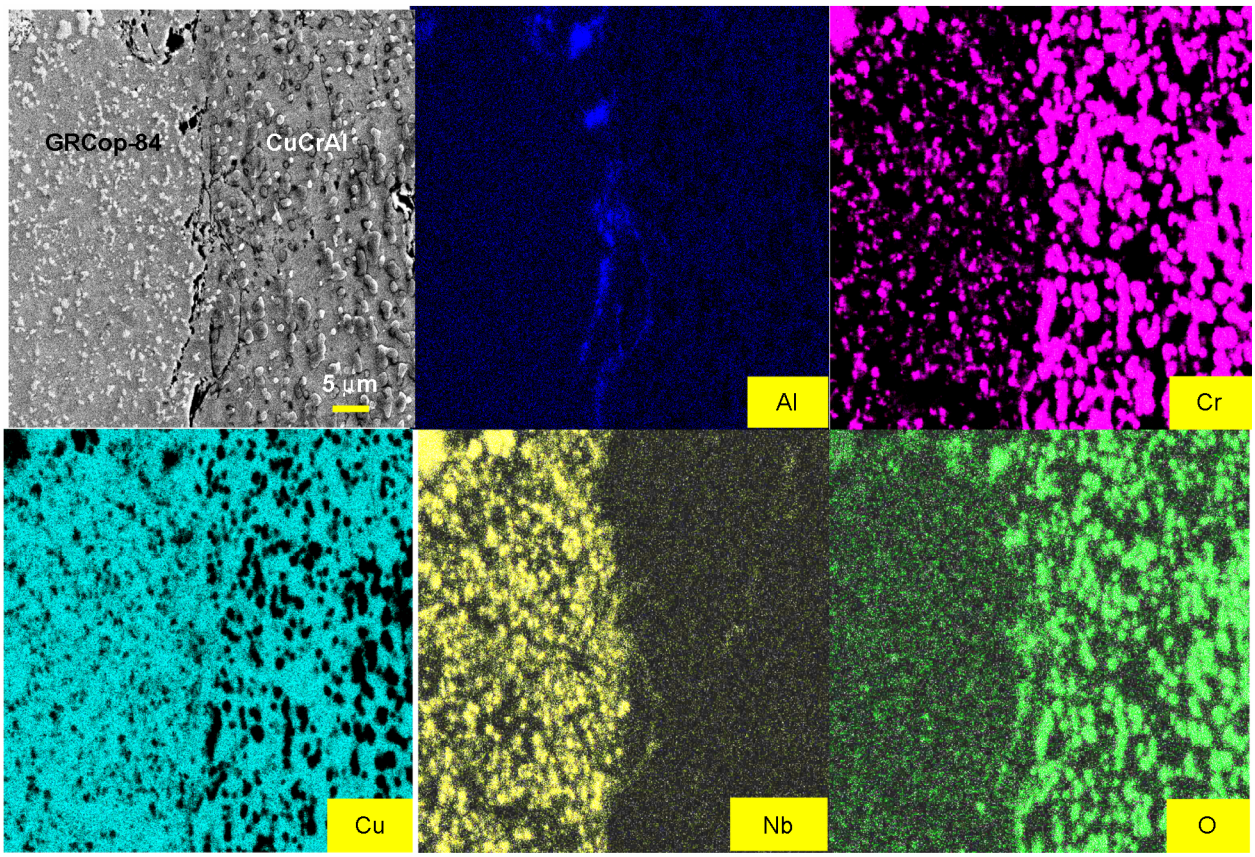

Figure 13.—Scanning electron micrograph and elemental dot maps from the polished cross-section of the Cu-23Cr-5Al coated GRCop-84 specimen cyclically oxidized at 1073 K for 80 cycles showing the distribution of Al, Cr, Cu, Nb and O across the

Scanning (fig. 14(a) and (c)) and backscattered (fig. 14(b) and (d)) electron microscopic observations of the cross-sections of the cyclically oxidized coated specimens showed several voids in the coatings. It was unclear whether these voids were present originally in the specimens prior to testing or whether they had developed during thermal cycling of the specimens. An examination of the coating-substrate interface revealed a general absence of voids. However, large number embedded alumina grit in the substrate and at the interface from the grit blasting of the surface prior to coating it (fig. 15). This is evident when the elemental dot maps for Al and O are compared with the secondary electron micrograph shown in figure 15. Also, the Cr and O elemental x-ray dot maps are fairly similar thereby suggesting that the initial Cr second phase particles in the coating have oxidized during cyclic oxidation. Additionally, the Al present in solid solution in the α-Cu matrix can preferentially react with any available oxygen and further reduce the activity of the oxygen in the matrix to below a critical value preventing the formation of copper oxides. Niu et al. (ref. 18) estimate that this critical partial pressure of oxygen is about 10^{-9} atm at 1073 K.

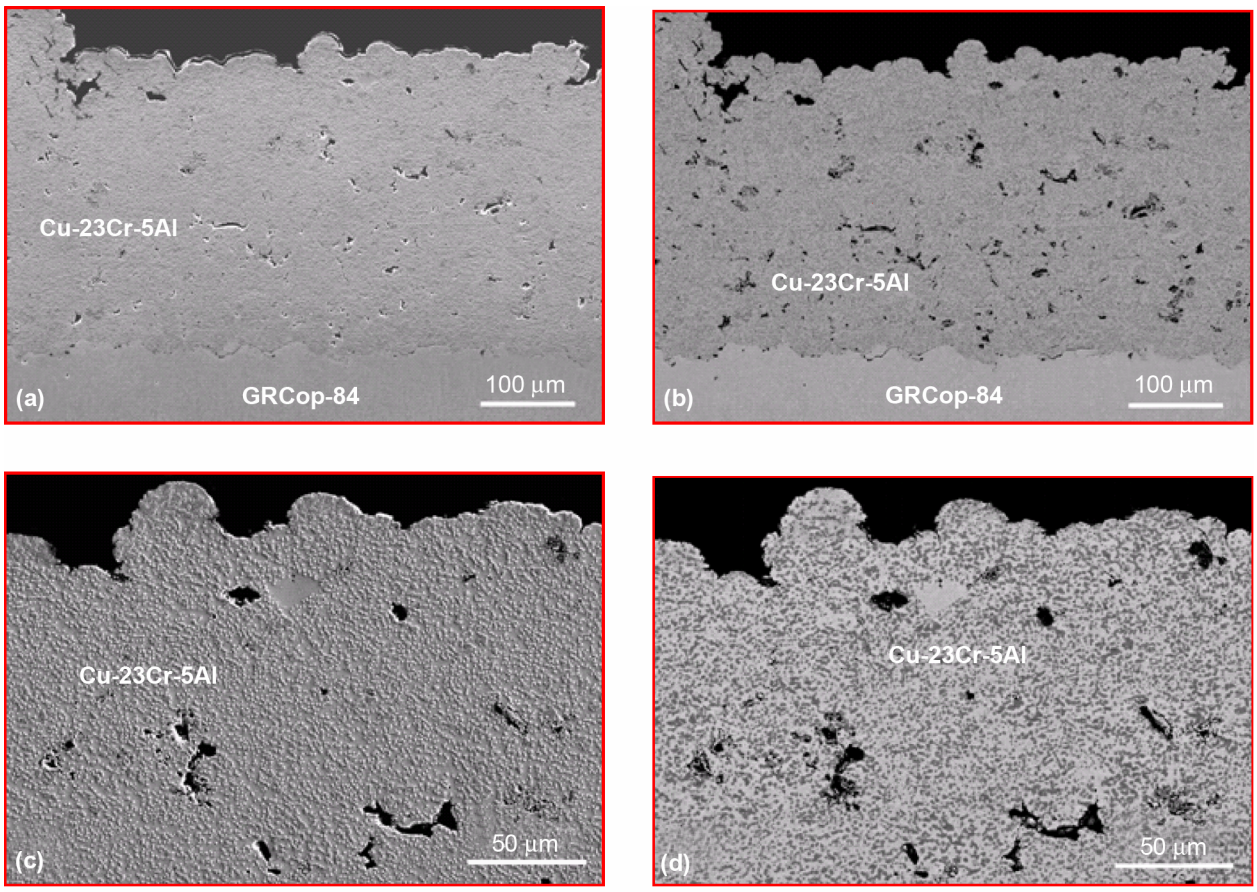

Figure 14.—(a) and (c) Scanning electron and (b) and (d) back scattered electron images of the cross-sections of a cold sprayed Cu-23Cr-5Al coated GRCop-84 specimen cyclically oxidized at 973 K for 1000 cycles.

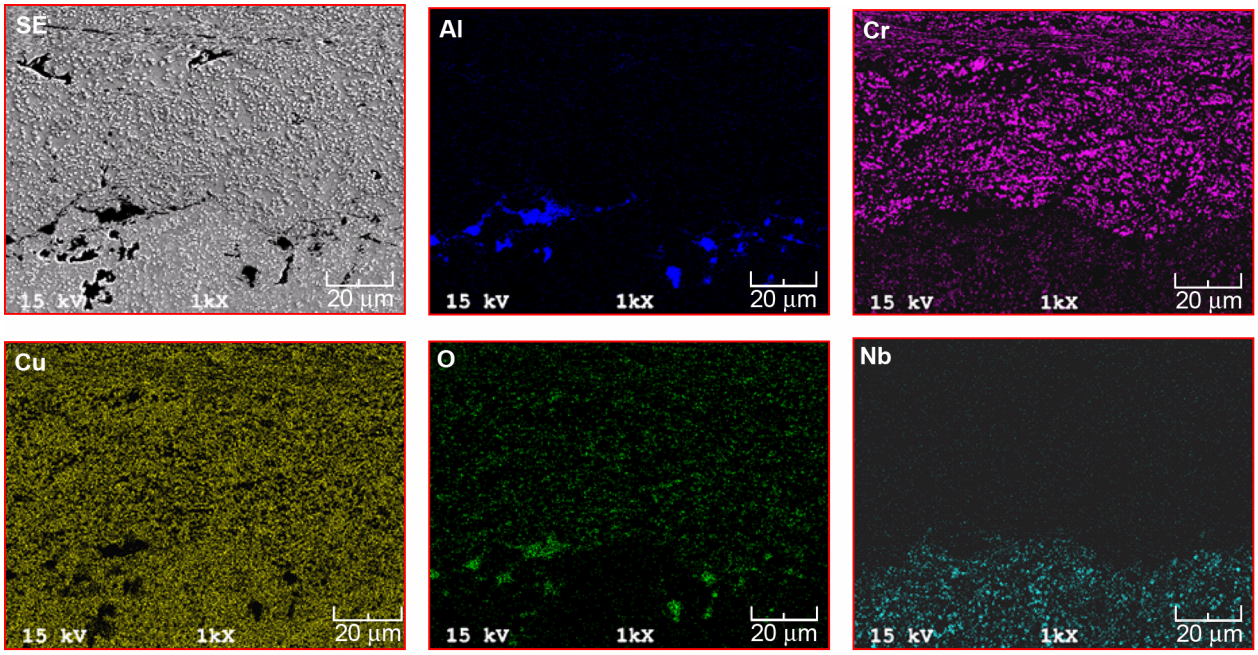

Figure 15.—Scanning electron image and elemental dot maps showing the presence of alumina grit particles at the Cu-23Cr-5Al/GRCop-84 interface in the specimen cyclically oxidized at 973 K for 1000 cycles.

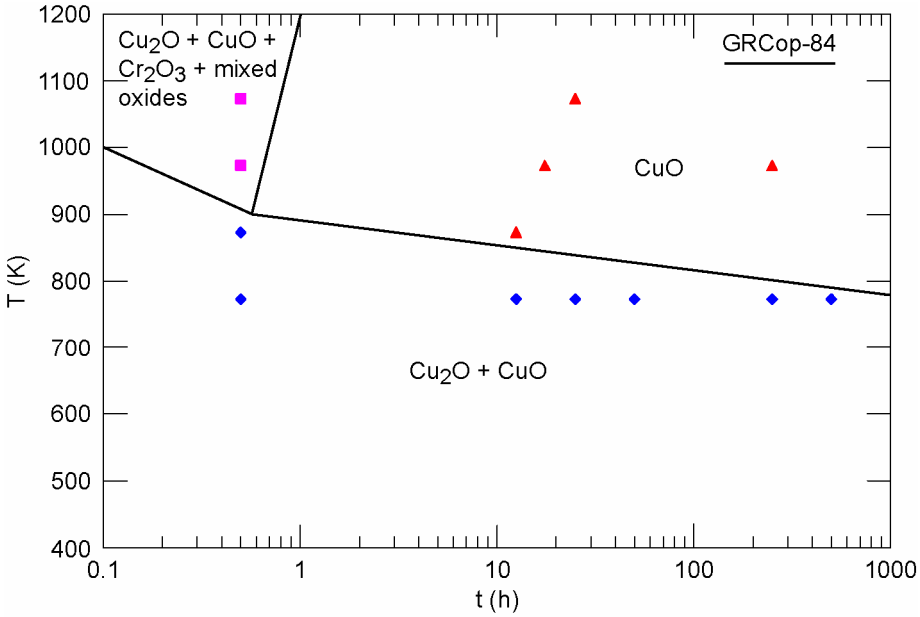

Figure 16.—Oxidation map for cyclically oxidized GRCop-84 plotted on absolute temperature-cumulative cyclic time space.

3.4 X-ray Diffraction Analyses

The XRD observations of the cyclically oxidized uncoated GRCop-84 specimens revealed that the compositions of the oxides in the scales varied with temperature and time. Figure 16 maps out the compositions of the surface oxides formed at different times during testing at each temperature. Both Cu_2O and CuO were observed at 773 K up through 1000 cycles corresponding to a cumulative time of 500 h. However, CuO was observed at temperatures above 773 K after 25 cycles corresponding to a cumulative time of 12.5 h. The transient oxides in the scales formed at 973 and 1073 K after 1 cycle corresponding to a cumulative time of 0.5 h consisted of a number of mixed oxides of Cu, Cr, and Nb with some exhibiting weak x-ray peaks. Interestingly, weak peaks denoting the presence of Cr_2O_3 were observed at both temperatures after 1 cycle but not after 25 cycles of testing.

3.5 Coating Behavior

It has been clearly demonstrated in this study that the cold sprayed CuCrAl coating alloy protects the GRCop-84 substrate up to temperatures as high as 1073 K (figs. 5 to 8) with no evidence of spallation (fig. 12(a) to (d)). An intriguing question is why does the coating perform so well? Based on the known oxidation behavior of the MCrAlY coatings, where M represents either Co, Fe or Ni, which form a continuous protective alumina scale, it is tempting to suggest that the CuCrAl alloys also forms a similar protective scale. A substantial amount of the Cr is in solid solution in the matrix in the MCrAlY alloys, where Al and Cr act synergistically to help form a continuous protective scale of alumina (ref. 19). However, since the Cr in the CuCrAl alloy is present almost entirely in the second phase due to its low solubility in Cu, it is uncertain whether this alloy will also form a protective alumina scale during oxidation. Although the XRD data of the exterior scale typically revealed strong β-Cr and α-Cu peaks, they did not show any alumina peaks. Figure 17 shows the SE image and the corresponding x-ray dot maps of the scale formed at the external surface of the oxidized Cu-23Cr-5Al coating. These observations clearly demonstrate that the scale is rich in Al, Cr, and O thereby suggesting that it consists of a mixed oxide. Therefore, it is reasonable to conclude that the Cu-23Cr-5Al forms a protective mixed oxide scale.

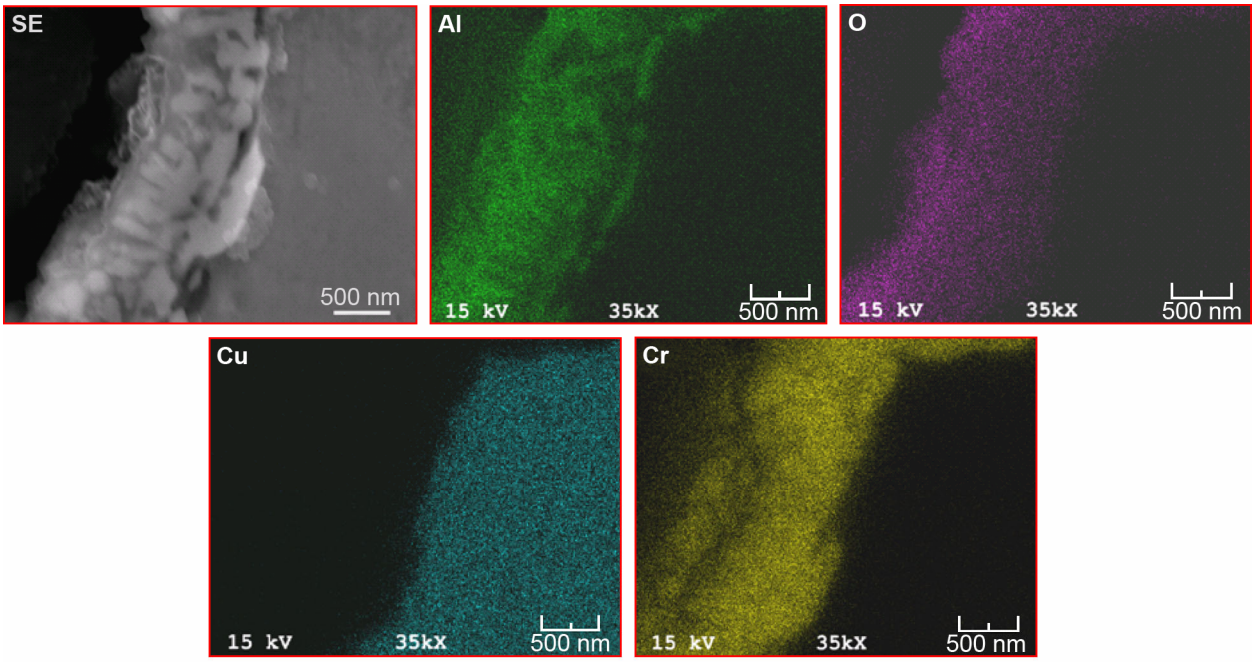

Figure 17.—X-ray dot maps determined from the boxed region in Figure 17 (b) showing the distribution of Al, Cr, Cu and O in the oxide scale of the Cu-23Cr-5Al coating after cyclic oxidation at 773 K for 1000 cycles.

Summary and Conclusions

A newly developed Cu-23 wt % Cr-5%Al coating was deposited on a GRCop-84 copper alloy substrate by the cold spray technique. The coating proved to be very effective in preventing the cyclic oxidation of the substrate in the temperature range 773 to 1073 K for up to 1000 cycles corresponding to a cumulative cyclic time of 500 h. No significant weight loss of the coated substrate was observed at 773 and 873 K after 1000 cycles but there was about 10 percent loss in weight at 973 K due to the oxidation of the uncoated sides. Similarly, the excessive oxidation of the uncoated sides resulted in about 10 percent loss in weight of the coated specimen at 1073 K after 40 cycles. In contrast, the uncoated specimen lost between 60 to 80 percent of its original weight at 773 and 973 K after 500 and 150 cycles, respectively. Cross-sectional microstructures of the coated and uncoated substrates revealed that the coating was intact at all the temperatures, whereas the uncoated GRCop-84 showed excessive spallation of the oxide scale. The uncoated substrate showed extensive oxidation at 1073 K. X-ray diffraction results revealed that Cu_2O and CuO were the two main oxides present in the external scale of the oxidized GRCop-84 under most test conditions although Cr_2O_3 and mixed oxides were detected at high temperatures and short cycle times. An experimental cyclic oxidation map showing the composition of the scale is presented. The x-ray data from the CuCrAl coating typically revealed α-Cu and β-Cr with little evidence of either Cu_2O or CuO. Elemental x-ray dot maps of the oxide scale formed on the CuCrAl coating revealed that it consisted of a mixture of aluminum and chromium oxides. It is concluded that the cold sprayed CuCrAl coating was very effective in protecting the GRCo-84 substrates.

References

1. R.J. Quentmeyer, “Experimental Fatigue Life Investigation of Cylindrical Thrust Chambers,” NASA TM X–73665, Lewis Research Center, OH (1977).

2. D.K. Huzel and D.H. Huang, "Modern Engineering for Design of Liquid-Propellant Rocket Engines," Progress in Astronautics and Aeronautics, vol. 147 (ed. A. R. Seebass), American Institute of Aeronautics and Astronautics, Inc., Washington, DC, pp. 67–134 (1992).
3. J. Singh, G. Jerman, B. Bhat, and R. Poorman, "Microstructural Stability of Wrought, Laser And Electron Beam Glazed NARloy-Z Alloy at Elevated Temperatures," NASA TM–108431, George C. Marshall Space Flight Center, Huntsville, AL, (1993).
4. H.J. Kasper, "Thrust Chamber Life Prediction," Advanced High Pressure O_2/H_2 Technology, NASA CP–2372 (eds. S.F. Morea and S.T. Wu), George C. Marshall Space Flight Center, Huntsville, AL, pp. 36–43 (1985).
5. R.J. Quentmeyer, "Rocket Thrust Chamber Thermal Barrier Coatings," Advanced High Pressure O_2/H_2 Technology, NASA CP–2372 (eds. S. F. Morea and S. T. Wu), George C. Marshall Space Flight Center, Huntsville, AL, pp. 49-58 (1985).
6. D.B. Morgan and A.C. Kobayashi, "Main Combustion Chamber and Cooling Technology Study—Final Report," NASA CR–184345, NASA Marshall Space Flight Center, Huntsville, AL (1989).
7. D. Ellis and D. Keller, NASA/CR—2000-210055, NASA Glenn Research Center, Cleveland, OH (2000).
8. R. Holmes, D. Ellis, and T. McKechnie, "Robust Low Cost Aerospike/RLV Combustion Chamber by Advanced Vacuum Plasma Process," Countdown to the Millennium Proceedings, 36th Space Congress, Canaveral Council of Technical Societies, Cape Canaveral, FL (1999).
9. R. Hickman, T. McKechnie and R. Holmes, "Material Properties of Vacuum Plasma Sprayed Cu-8Cr-4Nb for Liquid Rocket Engines," Paper No. AIAA–2001–3693, 37th AIAA/ASME/SAE/ASEE/Joint Propulsion Conference, Salt Lake City, UT, American Institute of Aeronautics and Astronautics, Inc., pp. 1–9 (2001).
10. K.T. Chiang, P.D. Krotz, and J.L. Yuen, Surf. Coat. Technol. **76**, pp. 14–19 (1995).
11. K.T. Chiang and J.P. Ampaya, Surf. Coat. Technol. **78**, pp. 243–247 (1996).
12. T.A. Wallace, R.K Clark and K.T. Chiang, J. Spacecraft Rockets **35**, pp. 546–51 (1998).
13. S. Elam, R. Holmes, T. McKechnie, R. Hickman and T. Pickens, "VPS GRCop-84 Chamber Liner Development Efforts," 52nd JANNAF Propulsion Meeting/1st Liquid Propulsion Subcommittee Meeting, Las Vegas, Chemical Propulsion Information Agency, The Johns Hopkins University, Baltimore, MD, pp. 1–10 (2004).
14. M.F. Smith, J.E. Brockmann, R.C. Dykhuizen, D.L. Gilmore, R.A. Neiser and T.J. Roemer, "Cold Spray Direct Fabrication—High Rate, Solid State, Material Consolidation," MRS Proceedings, vol. 542, Materials Research Society, Pittsburgh, PA, pp. 65–76 (1999).
15. J. Karthikeyan, "Cold Spray Technology," Advan. Mater. Process. **163**, pp. 33–35 (2005).
16. S.V. Raj, unpublished research, NASA Glenn Research Center, Cleveland, OH (2003).
17. K.T. Chiang and D.L. Grimmett, Proc. Electrochem. Soc. **98-9**, p. 489–499 (1998).
18. Y. Niu, F. Gesmundo, F. Viani and D.L. Douglass, Oxid. Met. **48** p. 357–380 (1997).
19. J.L. Smialek and G.H. Meier, *Superalloy II*, (edited by C.T. Sims, N.S. Stoloff, and W.C. Hagel), John Wiley, New York, pp. 293–326 (1987).

REPORT DOCUMENTATION PAGE

Form Approved
OMB No. 0704-0188

1. AGENCY USE ONLY (*Leave blank*)	2. REPORT DATE	3. REPORT TYPE AND DATES COVERED
	June 2006	Technical Memorandum

4. TITLE AND SUBTITLE

Cyclic Oxidation Behavior of Cold Sprayed CuCrAl-Coated and Uncoated GRCop-84 Substrates for Space Launch Vehicles

5. FUNDING NUMBERS

WBS–22–617–44–20

6. AUTHOR(S)

S.V. Raj, C. Barrett, J. Karthikeyan, and R. Garlick

7. PERFORMING ORGANIZATION NAME(S) AND ADDRESS(ES)

National Aeronautics and Space Administration
John H. Glenn Research Center at Lewis Field
Cleveland, Ohio 44135–3191

8. PERFORMING ORGANIZATION REPORT NUMBER

E–15625

9. SPONSORING/MONITORING AGENCY NAME(S) AND ADDRESS(ES)

National Aeronautics and Space Administration
Washington, DC 20546–0001

10. SPONSORING/MONITORING AGENCY REPORT NUMBER

NASA TM—2006-214350

11. SUPPLEMENTARY NOTES

S.V. Raj, C. Barrett, and R. Garlick, NASA Glenn Research Center; and J. Karthikeyan, ASB Industries, Inc., 1031 Lambert Street, Barberton, Ohio 44203–1689. Responsible person, S.V. Raj, organization code RXD, 216–433–8195.

12a. DISTRIBUTION/AVAILABILITY STATEMENT

Unclassified - Unlimited
Subject Categories: 15, 26, 23, and 20

Available electronically at http://gltrs.grc.nasa.gov

This publication is available from the NASA Center for AeroSpace Information, 301–621–0390.

12b. DISTRIBUTION CODE

13. ABSTRACT ***(Maximum 200 words)***

A newly developed Cu-23 (wt %) Cr-5%Al (CuCrAl) alloy shown to resist hydridation and oxidation in an as-cast form is currently being considered as a protective coating for GRCop-84, which is an advanced copper alloy containing 8 (at.%) Cr and 4 (at.%) Nb. The coating was deposited on GRCop-84 substrates by the cold spray deposition technique. Cyclic oxidation tests conducted in air on both coated and uncoated substrates between 773 and 1073 K revealed that the coating remained intact and protected the substrate up to 1073 K. No significant weight loss of the coated specimens were observed at 773 and 873 K even after a cumulative cyclic time of 500 h. About a 10 percent weight loss observed at 973 and 1073 K was attributed to the excessive oxidation of the uncoated sides. In contrast, the uncoated substrate lost as much as 80 percent of its original weight under similar test conditions. It is concluded that the cold sprayed CuCrAl coating is suitable for protecting GRCop-84 substrates.

14. SUBJECT TERMS

Cyclic oxidation; GRCop-84; Copper alloy; CuCrAl coating; Space launch vehicle

15. NUMBER OF PAGES

24

16. PRICE CODE

17. SECURITY CLASSIFICATION OF REPORT	18. SECURITY CLASSIFICATION OF THIS PAGE	19. SECURITY CLASSIFICATION OF ABSTRACT	20. LIMITATION OF ABSTRACT
Unclassified	Unclassified	Unclassified	